Journal of Quality Measurement and Analysis *JQMA* 12(1-2) 2016, 11-26
Jurnal Pengukuran Kualiti dan Analisis

PERFORMANCE COMPARISON OF THE EXACT RUN-LENGTH DISTRIBUTION BETWEEN THE RUN SUM $\bar{X}$ AND EWMA $\bar{X}$ CHARTS

(Perbandingan Prestasi antara Carta Hasil Tambah Larian $\bar{X}$ dan EWMA $\bar{X}$ Berdasarkan Taburan Panjang Larian Tepat)

J.K. CHONG[1], W.L. TEOH[1], MICHAEL B.C. KHOO[2], Z.L. CHONG[1] & S.Y. TEH[3]

ABSTRACT

The run sum (RS) $\bar{X}$ and exponentially weighted moving average (EWMA) $\bar{X}$ charts are very effective in detecting small and moderate process mean shifts. The design of the RS $\bar{X}$ and EWMA $\bar{X}$ charts based on the average run length (ARL) alone, can be misleading and confusing. This is due to the fact that the run-length distribution of a control chart is highly right-skewed when the process is in-control or slightly out-of-control; while that for the out-of-control cases, the run-length distribution is almost symmetric. On the other hand, the percentiles of the run-length distribution provide the probability of getting a signal by a certain number of samples. This will benefit practitioners as the percentiles of the run-length distribution give comprehensive information regarding the behaviour of a control chart. Accordingly, this paper provides a thorough study of the run-length properties (ARL, standard deviation of the run length and percentiles of the run-length distribution) for the RS $\bar{X}$ and EWMA $\bar{X}$ charts. Comparative studies show that the EWMA $\bar{X}$ chart outperforms the RS $\bar{X}$ charts for detecting small mean shifts when all the control charts are optimized with respect to a small shift size. However, the RS $\bar{X}$ charts surpass the EWMA $\bar{X}$ chart for all sizes of mean shifts when all the control charts are optimized with respect to a large shift size.

Keywords: average run length; EWMA $\bar{X}$ chart; percentiles of the run-length distribution; run sum $\bar{X}$ chart; standard deviation of the run length

ABSTRAK

Carta $\bar{X}$ hasil tambah larian (RS) dan $\bar{X}$ purata bergerak berpemberat eksponen (EWMA) adalah sangat berkesan untuk mengesan anjakan min proses yang kecil dan sederhana. Reka bentuk carta $\bar{X}$ RS dan $\bar{X}$ EWMA berdasarkan panjang larian purata (ARL) sahaja adalah mengelirukan. Hal ini kerana taburan panjang larian untuk carta kawalan adalah sangat terpencong ke kanan apabila proses berada dalam kawalan atau hanya sedikit di luar kawalan; manakala bagi kes di luar kawalan, taburan panjang larian adalah hampir simetri. Sebaliknya, persentil taburan panjang larian memberikan kebarangkalian untuk mendapat isyarat dengan bilangan sampel yang tertentu. Hal ini dapat memanfaatkan para pengamal kerana persentil taburan panjang larian memberi maklumat yang komprehensif tentang kelakuan carta kawalan. Oleh hal yang demikian, makalah ini memberikan kajian yang menyeluruh tentang sifat-sifat panjang larian (ARL, sisihan piawai panjang larian dan persentil taburan panjang larian) untuk carta $\bar{X}$ RS dan $\bar{X}$ EWMA. Perbandingan dalam kajian ini menunjukkan bahawa carta $\bar{X}$ EWMA adalah lebih baik daripada carta $\bar{X}$ RS untuk mengesan anjakan min yang kecil apabila semua carta kawalan itu dioptimumkan berdasarkan saiz anjakan yang kecil. Walau bagaimanapun, carta $\bar{X}$ RS adalah lebih baik daripada carta $\bar{X}$ EWMA bagi semua saiz anjakan min apabila semua carta kawalan itu dioptimum berdasarkan suatu saiz anjakan yang besar.

Kata kunci: panjang larian purata; carta $\bar{X}$ EWMA; persentil taburan panjang larian; carta $\bar{X}$ hasil tambah larian; sisihan piawai panjang larian

1. Introduction

Statistical Process Control (SPC) is a collection of statistical techniques to monitor and control a process. Control charts are applied to monitor the quality characteristics of products. The foremost objective of developing a control chart is to quickly detect the occurrence of process shifts; thus, necessary corrective actions can be taken before a large amount of nonconforming units are being manufactured (Montgomery 2013).

The performance of a control chart is usually based on the average run length (ARL) criterion, which is long recognised in SPC field. Interpretation of a control chart solely based on the ARL can be misleading to practitioners (Bischak & Trietsh 2007; Chakraborti 2007; Teoh *et al*. 2015). This is because the shape of the run-length distribution changes according to the magnitude of shifts. It changes from highly right-skewed when the shift is small to nearly symmetric when the shift is large. In general, the ARL only gives the expected number of samples to signal. It does not provide the probability of getting an out-of-control signal by a certain number of samples. On the other hand, the percentiles of the run-length distribution is more intuitive as they focus on the behaviour of the charts. Several studies have found that the percentiles of the run-length distribution provide a comprehensive interpretation regarding the exact run length, such as those by Khoo and Quah (2002), Khoo (2004), Radson and Boyd (2005), Shmueli and Cohen (2003), and Teoh *et al.* (2016). Palm (1990) claimed that the 50^{th} percentile of the run-length distribution (i.e. the median run length, MRL) represents half of the time. For example, the out-of-control MRL (MRL_1) of 30 indicates that 50% of all the run lengths are less than 30. Furthermore, the percentiles of the run-length distribution provide a practical guidance regarding the early false alarms and spread of the run-length distribution. To have a good understanding of a control chart, it is necessary to supplement the ARL with the percentiles of the run-length distribution and standard deviation of the run length (SDRL) (Jones 2002).

On a different note, the run sum (RS) chart was developed by Roberts (1966) to increase the sensitivity of the basic chart. The advantage of the RS chart is the great improvement of the detection speed, while maintaining the simplicity of the basic chart. Reynolds (1971) suggested to use the RS control chart with eight regions, where four regions are on each side of the centre line and scores are assigned for each region. Jaehn (1987) suggested that the zone control chart is a special case of the RS $\bar{X}$ chart. Davis *et al*. (1994) proposed a general model of the zone control chart with fast-initial-response (FIR) feature. Champ and Rigdon (1997) developed the ARL-based RS $\bar{X}$ chart by using the Markov chain approach. They concluded that the RS $\bar{X}$ chart offers better statistical efficiency than the Shewhart $\bar{X}$ chart with supplementary runs rules. Besides, they also indicated that by adding more regions and scores, the RS $\bar{X}$ chart is competitive in terms of detection speed, compared to the exponentially weighted moving average (EWMA) $\bar{X}$ and cumulative sum (CUSUM) $\bar{X}$ charts. Parkhideh and Parkhideh (1998) designed a flexible zone control chart for individual observation. Aguirre-Torres and Reyes-Lopez (1999) studied both the RS $\bar{X}$ and R charts. Davis and Krehbiel (2002) compared the performance of the Shewhart $\bar{X}$ chart with runs rules with that of the zone control chart when linear trend presents in the process. Acosta-Mejia and Pignatiello (2010) investigated the RS R control chart with FIR feature for monitoring the process dispersion. The RS t chart, which is more robust against changes in the process variance compared to the RS $\bar{X}$ chart, was studied by Sitt *et al*. (2014). Acosta-Mejia and Rincon (2014) introduced the continuous RS chart, which has a centre line equal to zero and scores equal to the standardized subgroup means. Recently, Teoh *et al.* (2017) developed the run sum charts for monitoring the coefficient of variation, which broaden the charting capability to various scientific and societal applications.

Another type of control chart, called the EWMA chart, was introduced by Roberts (1959). A considerable amount of literature on EWMA control charts have been conducted over the years. Crowder (1987) formulated the EWMA chart properties by using integral equations. The optimal design of the EWMA chart based on ARL was further discussed by Crowder (1989). Lucas and Saccucci (1990) adopted the Markov chain approach to compute the run-length properties of the EWMA control chart. Gan (1993) developed the optimal MRL-based EWMA control chart. Steiner (1999) proposed the FIR-EWMA control charts with time-varying control limits. Moreover, Jones (2002) investigated the effect of parameters estimation on the EWMA $\bar{X}$ chart. Shu *et al*. (2007) studied the two one-sided EWMA charts for upward and downward changes in the process mean. Some recent studies on the EWMA control charts can be found in Abdul *et al*. (2015), Castagliola *et al*. (2011), Khan *et al*. (2016), Khoo *et al.* (2016) and Zhang *et al*. (2009).

To date, none of the existing literature compares the RS $\bar{X}$ and EWMA $\bar{X}$ charts, in terms of the percentiles of the run-length distribution. The percentiles of the run-length distribution are more credible compared to the ARL, especially when the skewness of the associated run-length distribution is different for different shifts. Therefore, the objective of this paper is to thoroughly examine and compare the ARL, SDRL and percentiles of the run-length distribution for both the RS $\bar{X}$ and EWMA $\bar{X}$ charts. The structure of this paper is as follows: Sections 2 and 3 introduce the RS $\bar{X}$ and EWMA $\bar{X}$ charts. In Section 4, the comparison of the ARL, SDRL and percentiles of the run length distribution are investigated. Finally, some conclusions are drawn in Section 5.

2. The RS $\bar{X}$ chart

Let $\{X_{i,1}, X_{i,2},\ldots, X_{i,n}\}$ be the i^{th} sample, where i = 1, 2, … and n is the number of observations. Assume that the j^{th} (for $j = 1, 2, \ldots, n$) quality characteristic in sample i follows a normal distribution, i.e. $X_{i,j} \sim N\left(\mu_0 + \delta\sigma_0, \sigma_0^{\,2}\right)$. Here, μ_0 is the in-control mean and σ_0 is the in-control standard deviation. The magnitude of a mean shift in multiples of the standard deviation is denoted as δ. The process is statistically in-control when $\delta = 0$ and out-of-control when $\delta \neq 0$. Also, assume that there is independence between and within samples.

The RS $\bar{X}$ chart is divided into k regions above and k regions below the central line (CL). Figure 1 graphically shows the k regions RS $\bar{X}$ chart with the associated scores, probabilities and control limits. The integer scores $\left(0 \leq S_1 \leq S_2 \leq \ldots \leq S_k\right)$ and $\left(-S_k \leq -S_{k-1} \leq \ldots \leq -S_2 \leq -S_1 \leq 0\right)$ are assigned to each of the regions above and below the CL, respectively. From Figure 1, the regions and probabilities above the CL are $\left(R_{+1}, R_{+2}, \ldots, R_{+k}\right)$ and $\left(p_{+1}, p_{+2}, \ldots, p_{+k}\right)$, respectively; while the regions and probabilities below the CL are $\left(R_{-1}, R_{-2}, \ldots, R_{-k}\right)$ and $\left(p_{-1}, p_{-2}, \ldots, p_{-k}\right)$, respectively. Note that $CL = \mu_0$ and k is the number of regions desired. In this paper, we consider $k \in \{4, 7\}$. Champ and Rigdon (1997), Sitt *et al.* (2014), and Teoh *et al.* (2017) also considered $k \in \{4, 7\}$. The k regions RS $\bar{X}$ chart at the i^{th} sample is defined by the following upper $\left(U_i\right)$ and lower $\left(L_i\right)$ cumulative sums:

$$U_i = \begin{cases} U_{i-1} + S\left(\bar{X}_i\right), & \text{if } \bar{X}_i \geq \mu_0 \\ 0, & \text{if } \bar{X}_i < \mu_0 \end{cases}, \tag{1}$$

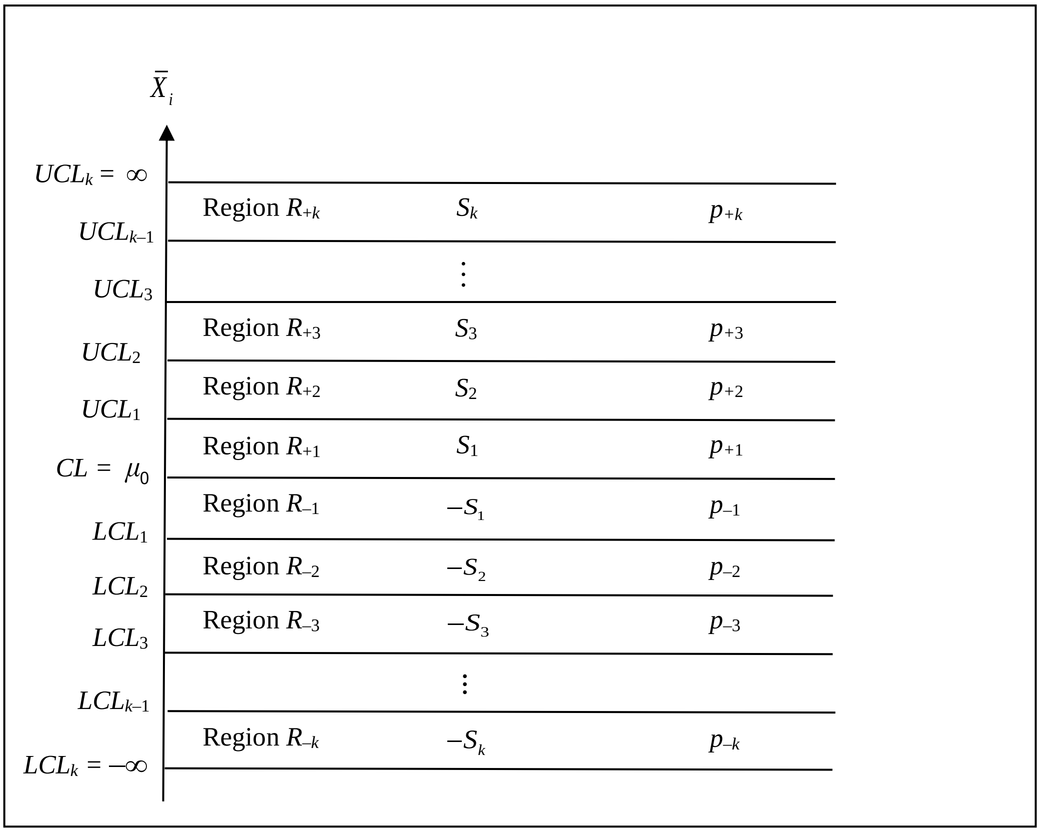

Figure 1: Graphical view of the *k* regions above and *k* regions below the *CL* of the RS $\bar{X}$ chart with the associated scores, probabilities and control limits

and

$$L_i = \begin{cases} L_{i-1} + S\left(\bar{X}_i\right), & \text{if } \bar{X}_i \le \mu_0 \\ 0, & \text{if } \bar{X}_i > \mu_0 \end{cases}, \tag{2}$$

where $U_0 = L_0 = 0$. In Equations (1) and (2), $S\left(\bar{X}_i\right)$ is the score function, where $S\left(\bar{X}_i\right) = S_t$ when $\bar{X}_i \in R_{+t}$ and $S\left(\bar{X}_i\right) = -S_t$ when $\bar{X}_i \in R_{-t}$, for $t =$ 1, 2, …, *k*. The upper $\left(UCL_1 < UCL_2 < \ldots < UCL_{k-1} < UCL_k = \infty\right)$ and lower $\left(-\infty = LCL_k < LCL_{k-1} < \ldots < LCL_2 < LCL_1\right)$ control limits of the *k* regions RS $\bar{X}$ chart are computed as

$$UCL_t = \mu_0 + K\left(\frac{3t}{k-1}\right)\frac{\sigma_0}{\sqrt{n}} \tag{3}$$

and

$$LCL_t = \mu_0 - K\left(\frac{3t}{k-1}\right)\frac{\sigma_0}{\sqrt{n}}, \tag{4}$$

respectively, where $t = 1, 2, \ldots, k$ and K is the control limits' parameter.

The procedure of constructing the k regions RS $\bar{X}$ chart is as follows (Champ & Rigdon 1997):

(1) Determine the number of regions k, scores $\pm S_t$, control limits UCL_t and LCL_t, based on an optimal design of the chart.
(2) Collect a sample, each having n observations and compute the sample mean, $\bar{X}_i = \sum_{i=1}^{n} X_i / n$.
(3) Start with the cumulative score at 0, i.e. $(U_0, L_0) = (+0, -0)$.
(4) Accumulate the scores U_i and L_i corresponding to the regions R_{+t} and R_{-t}, respectively, in which the sample mean, $\bar{X}_i$ falls (refer to Equations (1) and (2)).
(5) Reset the cumulative scores of U_i or L_i to zero if $\bar{X}_i$ falls on the other side of the CL, i.e, $\bar{X}_i < \mu_0$ (refer to Equation (1)) or $\bar{X}_i > \mu_0$ (refer to Equation (2)), respectively.
(6) Declare the process as out-of-control if a positive cumulative score $U_i \geq S_k$ or a negative cumulative score $L_i \leq -S_k$, where S_k is the triggering score which serves as a boundary beyond which the chart will signal an out-of-control.

For example, the probabilities p_{+2} and p_{+3} in regions R_{+2} and R_{+3}, respectively, (refer to Figure 1) can be obtained by using Equations (5) and (6), as follows (Champ & Ridgon 1997):

$$\begin{aligned} p_{+2} &= P\left(UCL_1 \leq \bar{X}_i < UCL_2\right) \\ &= P\left[\mu_0 + K\left(\frac{3}{k-1}\right)\frac{\sigma_0}{\sqrt{n}} \leq \bar{X}_i < \mu_0 + K\left(\frac{6}{k-1}\right)\frac{\sigma_0}{\sqrt{n}}\right] \\ &= \Phi\left[K\left(\frac{6}{k-1}\right) - \delta\sqrt{n}\right] - \Phi\left[K\left(\frac{3}{k-1}\right) - \delta\sqrt{n}\right], \end{aligned} \tag{5}$$

and

$$\begin{aligned} p_{+3} &= P\left(UCL_2 \leq \bar{X}_i < UCL_3\right) \\ &= P\left[\mu_0 + K\left(\frac{6}{k-1}\right)\frac{\sigma_0}{\sqrt{n}} \leq \bar{X}_i < \mu_0 + K\left(\frac{9}{k-1}\right)\frac{\sigma_0}{\sqrt{n}}\right] \\ &= \Phi\left[K\left(\frac{9}{k-1}\right) - \delta\sqrt{n}\right] - \Phi\left[K\left(\frac{6}{k-1}\right) - \delta\sqrt{n}\right], \end{aligned} \tag{6}$$

where $\Phi(.)$ is the cumulative distribution function (cdf) of the standard normal distribution. The probabilities $p_{\pm t}$, for other values of t, can be computed using the same method as displayed in Equations (5) and (6).

Suppose that we have a discrete-time Markov chain with $p + 1$ states, where states $1, 2, \ldots, p$ are transient and the state $p + 1$ is an absorbing state. Here, p is the number of possible ordered pairs (U_i, L_i) when the process is in-control. The transition probability matrix **P** of the discrete-time Markov chain has the following structure:

$$\mathbf{P} = \begin{pmatrix} \mathbf{Q} & \mathbf{r} \\ \mathbf{0}^T & 1 \end{pmatrix}, \tag{7}$$

where **Q** is the ($p \times p$) transient-probability matrix, $\mathbf{0} = (0, 0, \ldots, 0)^T$ and **r** is the ($p \times 1$) vector that satisfies $\mathbf{r} = \mathbf{1} - \mathbf{Q1}$ (i.e. the row probabilities must sum to 1), with $\mathbf{1} = (1, 1, \ldots, 1)^T$. Note that the dimension and generic elements of matrix **Q** for the k regions RS $\bar{X}$ chart depend on the choice of the scores $\{S_1, S_2, \ldots, S_k\}$. The matrix **Q** does not have a general form. Refer to Teoh *et al*. (2017) for the detailed procedure for obtaining matrix **Q**.

The computation of the ARL by using the Markov chain approach is as follows:

$$\text{ARL} = \mathbf{s}^T (\mathbf{I} - \mathbf{Q})^{-1} \mathbf{1}, \tag{8}$$

where $\mathbf{s} = (1, 0, \ldots, 0)^T$ is the vector of initial probability having a unity in the first element and zeros elsewhere; while **I** is the ($p \times p$) identity matrix. Also, the computation of the SDRL by means of the Markov chain approach is calculated as

$$\text{SDRL} = \sqrt{2\mathbf{s}^T (\mathbf{I} - \mathbf{Q})^{-2} \mathbf{Q1} - \text{ARL}^2 + \text{ARL}}\ . \tag{9}$$

Let N denotes the run length for the k regions RS $\bar{X}$ chart. The cdf of N, $F_N(\ell)$ for the k regions RS $\bar{X}$ chart is calculated as

$$F_N(\ell) = P(N \le \ell) = \mathbf{s}^T (\mathbf{I} - \mathbf{Q}^{\ell}) \mathbf{1}, \tag{10}$$

where $\ell \in \{1, 2, \ldots\}$. The $(100\gamma)^{\text{th}}$ percentiles of the run-length distribution can be determined as the value ℓ_γ such that (Gan 1993)

$$P(N \le \ell_\gamma - 1) \le \gamma \ \text{ and } \ P(N \le \ell_\gamma) > \gamma, \tag{11}$$

where γ is in the range of $0 < \gamma < 1$. For example, the 30th percentile of the run-length distribution can be obtained from both Equations (10) and (11) by setting $\gamma = 0.3$ in Equation (11).

3. The EWMA $\bar{X}$ chart

The plotting statistic Z_i of the EWMA $\bar{X}$ chart is as follows (Crowder 1989):

$$Z_i = \lambda \bar{X}_i + (1 - \lambda) Z_{i-1}, \ \text{for } i = 1, 2, \ldots, \tag{12}$$

where λ $(0 < \lambda \le 1)$ is the smoothing constant, $\bar{X}_i$ is the i^{th} sample mean and $Z_0 = \mu_0$. The upper (UCL) and lower (LCL) control limits of the EWMA $\bar{X}$ chart are computed as follows:

$$UCL = \mu_0 + H\sigma_0, \tag{13}$$

and

$$LCL = \mu_0 - H\sigma_0 , \quad (14)$$

where $H = h\sqrt{\lambda/[n\ (2-\lambda)]}$ with the multiplier *h* controlling the width of the control limits. The EWMA $\bar{X}$ chart signals an out-of-control situation if $Z_i > UCL$ or $Z_i < LCL$. The ARL and SDRL of the EWMA $\bar{X}$ chart can be computed by using Equations (8) and (9), respectively. Similarly, the percentiles of the run-length distribution for the EWMA $\bar{X}$ chart can be computed from both Equations (10) and (11). Note that the details of the matrices **s** and **Q** in Equations (8), (9) and (10) are given Zhang *et al*. (2009).

4. Performance Comparison

In this section, we discuss the entire run-length distributions of the ARL-based optimal RS $\bar{X}$ and optimal EWMA $\bar{X}$ charts with specific ranges of $\delta \in \{0.00, 0.25, 0.50, 0.75, 1.00, 1.50, 2.00\}$ and $n \in \{3, 5, 7, 9\}$. Also, throughout this paper, we specify a fixed ARL_0 = 500 and $\delta_{opt} \in \{0.5, 1.5\}$, where ARL_0 is the in-control ARL and δ_{opt} is the desired mean shift, for which a quick detection is intended.

Tables 1 to 4 present the entire run-length profiles for the 4 and 7 regions RS $\bar{X}$ charts when ARL_0 = 500, $n \in \{3, 5, 7, 9\}$ and $\delta_{opt} \in \{0.5, 1.5\}$; while the corresponding run-length profiles of the EWMA $\bar{X}$ chart are shown in Tables 5 and 6. From Tables 1 to 4, the optimal charts' parameters (K, S_1, S_2, S_3, S_4) and (K, S_1, S_2, S_3, S_4, S_5, S_6, S_7) of the 4 and 7 regions RS $\bar{X}$ charts are obtained by minimizing the out-of-control ARL (ARL_1), subject to a desired ARL_0 value. Champ and Rigdon (1997) presented the details of the optimization algorithm of the RS $\bar{X}$ chart. Similarly, Tables 5 and 6 present the optimal chart's parameters (λ, H) of the EWMA $\bar{X}$ chart by minimizing the ARL_1, subject to a desired ARL_0 value. A study by Gan (1993) gives the details of the optimization algorithm of the EWMA $\bar{X}$ chart.

Tables 1 to 6 provide sufficient evidence to clarify that the ARL is a confusing measure. For example, the ARL_0 of 500 only provides us with the expected number of samples to signal. The ARL_0 does not provide a comprehensive measure regarding the probability of getting a false alarm by a certain sample. Therefore, there may exist a risk that a practitioner falsely interprets a control chart with half of the time that a signal will be detected by the 500th sample. But in actual scenario, a false alarm will be noticed earlier, i.e. by the 348th sample (the 50th percentile of the run length distribution is 348) with half of the time for all $n \in \{3, 5, 7, 9\}$ (see Table 1). For such a case, it is important to note that the MRL (i.e. the 50th percentile of the run-length distribution) is a better representative of central tendency of the run-length distribution compared to the ARL (Chakraborti 2007). If MRL_0 = 500, a practitioner may claim with 50% certainty that a false alarm will occur by the 500th sample. Here, MRL_0 is the in-control MRL.

The results in Tables 1 to 6 show that there is a great difference between ARLs and MRLs, especially when the process is in-control ($\delta = 0$) or if the shift is small; while this difference is small when the shift is large. This shows that the shape of the run-length distribution changes according to the magnitude of shifts, i.e. from highly right skewed when the shift is small to almost symmetric when the shift is large. Also, this implies that for a right-skewed distribution, the ARL is larger than the MRL; while the ARL is almost the same as the MRL in an almost symmetric distribution. Therefore, interpretation based on ARL alone is confusing. This is because interpretation based on ARL for a highly right-skewed distribution is surely different with that of an almost symmetric distribution. For a comprehensive understanding of a control chart, a practitioner cannot solely depend on the ARL, where the ARL needs to be supplemented with the MRL and percentiles of the run-length distribution.

The percentiles of the run-length distribution allow a practitioner to state with an exact probability that a chart will signal by a certain sample, regardless of the shift sizes. The computation of the higher percentiles (i.e. 80th, 90th and 95th) of the run-length distribution provides some critical and important information to practitioners. For instance, by referring to Table 4, when n = 9 and $\delta = 0.75$, practitioners will have 90% confident that an out-of-control signal will be detected by the 8th sample. The computation of the lower percentiles (i.e. 5th, 10th and 25th) of the run-length distribution when $\delta = 0$, provides an analysis regarding the early false alarm in a process. For example, in the case of the 4 regions RS $\bar{X}$ chart with $\delta_{\text{opt}} = 1.5$

Table 1: Exact ARL, SDRL and percentiles of the run-length distribution for the 4 regions RS $\bar{X}$ chart with optimal parameters (K, S_1, S_2, S_3, S_4), when $n \in \{3, 5, 7, 9\}$, $\delta_{\text{opt}} =$ 0.5 and ARL$_0$ = 500

δ	ARL	SDRL	Percentiles of the run-length distribution												
			5th	10th	20th	25th	30th	40th	50th	60th	70th	75th	80th	90th	95th
n = 3, (K, S_1, S_2, S_3, S_4) = (1.2432, 0, 3, 5, 10)															
0.00	500.00	496.28	29	56	115	147	181	257	348	458	601	692	802	1146	1490
0.25	87.32	83.26	8	13	23	28	34	47	62	80	104	119	138	196	253
0.50	18.65	15.00	4	5	7	8	9	11	14	17	22	24	28	38	49
0.75	7.90	4.83	3	3	4	5	5	6	7	8	9	10	11	14	17
1.00	4.81	2.27	2	3	3	3	4	4	4	5	5	6	6	8	9
1.50	2.70	1.05	1	1	2	2	2	2	3	3	3	3	3	4	4
2.00	1.79	0.74	1	1	1	1	1	2	2	2	2	2	2	3	3
n = 5, (K, S_1, S_2, S_3, S_4) = (1.2432, 0, 3, 5, 10)															
0.00	500.00	496.28	29	56	115	147	181	257	348	458	601	692	802	1146	1490
0.25	51.00	47.01	6	9	15	18	21	28	37	47	61	69	80	112	145
0.50	10.65	7.34	3	4	5	6	6	7	9	10	12	14	15	20	25
0.75	5.06	2.46	2	3	3	3	4	4	5	5	6	6	7	8	10
1.00	3.31	1.32	1	2	2	3	3	3	3	3	4	4	4	5	6
1.50	1.88	0.78	1	1	1	1	1	2	2	2	2	2	3	3	3
2.00	1.24	0.45	1	1	1	1	1	1	1	1	1	1	2	2	2
n = 7, (K, S_1, S_2, S_3, S_4) = (1.2432, 0, 3, 5, 10)															
0.00	500.00	496.28	29	56	115	147	181	257	348	458	601	692	802	1146	1490
0.25	34.81	30.91	5	7	11	13	15	20	25	32	41	47	54	75	96
0.50	7.63	4.60	3	3	4	5	5	6	6	7	9	9	10	14	17
0.75	3.92	1.66	2	2	3	3	3	3	4	4	4	5	5	6	7
1.00	2.63	1.02	1	1	2	2	2	2	3	3	3	3	3	4	4
1.50	1.46	0.59	1	1	1	1	1	1	1	2	2	2	2	2	3
2.00	1.06	0.24	1	1	1	1	1	1	1	1	1	1	1	1	2
n = 9, (K, S_1, S_2, S_3, S_4) = (1.2432, 0, 3, 5, 10)															
0.00	500.00	496.28	29	56	115	147	181	257	348	458	601	692	802	1146	1490
0.25	26.01	22.21	5	6	9	10	12	15	19	24	31	35	40	55	70
0.50	6.09	3.28	3	3	4	4	4	5	5	6	7	7	8	10	12
0.75	3.28	1.30	1	2	2	3	3	3	3	3	4	4	4	5	6
1.00	2.21	0.88	1	1	1	2	2	2	2	2	3	3	3	3	4
1.50	1.23	0.44	1	1	1	1	1	1	1	1	1	1	2	2	2
2.00	1.01	0.11	1	1	1	1	1	1	1	1	1	1	1	1	1

and n = 5, there is a 10% chance or 0.1 probability that a false alarm will occur by the 54th sample (see Table 2). According to Chakraborti (2007), the difference between the 5th and 75th (or 5th and 95th) percentiles of the run-length distribution describes the spread and variation of the run-length distribution. Let us denote $\ell_{0.75} - \ell_{0.25}$ $\left(\ell_{0.95} - \ell_{0.05}\right)$ as the difference between the 25th and 75th (5th and 95th) percentiles of the run-length distribution. Here, $\ell_{0.05}$, $\ell_{0.25}$, $\ell_{0.75}$ and $\ell_{0.95}$ are the 5th, 25th, 75th and 95th percentiles of the run-length distribution. For example, for the 7 regions RS $\bar{X}$ chart, the value of $\ell_{0.95} - \ell_{0.05}$ is quite large, i.e. 1467 when $\delta_{\text{opt}} = 1.5$,

Table 2: Exact ARL, SDRL and percentiles of the run-length distribution for the 4 regions RS $\bar{X}$ chart with optimal parameters (K, S_1, S_2, S_3, S_4), when $n \in \{3,\ 5,\ 7,\ 9\}$, δ_{opt} = 1.5 and ARL_0 = 500

			Percentiles of the run-length distribution												
δ	ARL	SDRL	5th	10th	20th	25th	30th	40th	50th	60th	70th	75th	80th	90th	95th
n = 3, (K, S_1, S_2, S_3, S_4) = (1.0810, 0, 0, 1, 2)															
0.00	500.00	498.69	27	54	113	145	179	256	347	458	602	693	804	1150	1495
0.25	156.65	154.71	10	18	36	46	57	81	109	144	188	216	251	358	465
0.50	33.89	31.44	4	6	10	12	14	19	24	31	40	46	53	75	97
0.75	11.43	9.17	2	3	4	5	6	7	9	11	14	15	17	23	30
1.00	5.64	3.89	1	2	3	3	3	4	5	6	7	7	8	11	13
1.50	2.41	1.32	1	1	1	1	2	2	2	2	3	3	3	4	5
2.00	1.49	0.66	1	1	1	1	1	1	1	2	2	2	2	2	3
n = 5, (K, S_1, S_2, S_3, S_4) = (1.0810, 0, 0, 1, 2)															
0.00	500.00	498.69	27	54	113	145	179	256	347	458	602	693	804	1150	1495
0.25	97.16	95.02	7	12	23	30	36	51	68	89	117	134	155	221	287
0.50	17.01	14.60	2	4	6	7	8	10	13	16	20	23	26	36	46
0.75	6.08	4.27	1	2	3	3	3	4	5	6	7	8	9	12	14
1.00	3.24	1.94	1	1	2	2	2	2	3	3	4	4	5	6	7
1.50	1.57	0.71	1	1	1	1	1	1	1	2	2	2	2	2	3
2.00	1.11	0.32	1	1	1	1	1	1	1	1	1	1	1	2	2
n = 7, (K, S_1, S_2, S_3, S_4) = (1.0323, 0, 0, 1, 3)															
0.00	500.00	499.21	26	53	112	144	179	256	347	458	602	693	804	1150	1496
0.25	97.53	95.61	7	12	23	29	36	51	68	90	117	134	156	222	288
0.50	13.77	11.03	2	3	5	6	7	9	11	13	16	18	21	28	35
0.75	4.87	3.18	1	1	2	3	3	4	4	5	6	7	7	9	11
1.00	2.57	1.56	1	1	1	1	1	2	2	3	3	3	4	5	5
1.50	1.23	0.51	1	1	1	1	1	1	1	1	1	1	1	2	2
2.00	1.01	0.12	1	1	1	1	1	1	1	1	1	1	1	1	1
n = 9, (K, S_1, S_2, S_3, S_4) = (1.5451, 0, 0, 1, 1)															
0.00	500.00	499.45	26	53	112	144	179	256	347	458	602	693	804	1151	1497
0.25	103.11	102.61	6	11	23	30	37	53	72	95	124	143	166	237	308
0.50	17.89	17.38	1	2	4	6	7	9	13	16	21	25	28	41	53
0.75	4.99	4.46	1	1	1	2	2	3	4	5	6	7	8	11	14
1.00	2.15	1.58	1	1	1	1	1	1	2	2	2	3	3	4	5
1.50	1.09	0.31	1	1	1	1	1	1	1	1	1	1	1	1	2
2.00	1.00	0.04	1	1	1	1	1	1	1	1	1	1	1	1	1

n = 3 and $\delta = 0$ (see Table 4). This illustrates that the run length has a large variation because of the long right tail when $\delta = 0$. Generally, the difference between these two percentiles of the run-length distribution decreases as n and δ increase.

When comparing the control charts' performance, a control chart having the smallest ARL_1, $SDRL_1$, MRL_1, $\ell_{0.75} - \ell_{0.25}$ and $\ell_{0.95} - \ell_{0.05}$, is deemed as the best chart. Here, ARL_1, $SDRL_1$ and MRL_1 represent the out-of-control ARL, SDRL, MRL, respectively. From Tables 1, 3 and 5 (i.e. when $\delta_{\text{opt}} = 0.5$) , it is obvious that the EWMA $\bar{X}$ chart has the smallest ARL_1,

Table 3: Exact ARL, SDRL and percentiles of the run-length distribution for the 7 regions RS $\bar{X}$ chart with optimal parameters (K, S_1, S_2, S_3, S_4, S_5, S_6, S_7), when $n \in \{3, 5, 7, 9\}$, δ_{opt} = 0.5 and ARL_0 = 500

			Percentiles of the run-length distribution												
δ	ARL	SDRL	5th	10th	20th	25th	30th	40th	50th	60th	70th	75th	80th	90th	95th
n = 3, (K, S_1, S_2, S_3, S_4, S_5, S_6, S_7) = (1.4687, 0, 1, 2, 3, 4, 5, 8)															
0.00	500.00	495.03	30	57	115	147	182	258	348	459	601	691	802	1145	1488
0.25	75.81	71.10	8	12	21	25	30	41	54	70	90	103	119	168	218
0.50	17.13	13.12	5	6	7	8	9	11	13	16	20	22	25	34	43
0.75	7.77	4.36	3	4	5	5	5	6	6	7	9	9	10	13	16
1.00	4.97	2.05	3	3	3	4	4	4	5	5	5	6	6	7	9
1.50	3.03	0.90	2	2	2	3	3	3	3	3	3	3	4	4	4
2.00	2.15	0.71	1	1	2	2	2	2	2	2	3	3	3	3	3
n = 5, (K, S_1, S_2, S_3, S_4, S_5, S_6, S_7) = (1.3554, 0, 1, 2, 4, 5, 7, 10)															
0.00	500.00	495.43	30	57	115	147	181	258	348	458	601	691	802	1145	1489
0.25	45.89	41.55	6	9	14	16	19	26	33	42	54	62	71	100	129
0.50	10.18	6.70	3	4	5	6	6	7	8	10	12	13	14	19	23
0.75	5.04	2.29	2	3	3	3	4	4	5	5	6	6	6	8	9
1.00	3.39	1.21	2	2	3	3	3	3	3	3	4	4	4	5	6
1.50	2.02	0.73	1	1	1	2	2	2	2	2	2	2	3	3	3
2.00	1.35	0.50	1	1	1	1	1	1	1	1	2	2	2	2	2
n = 7, (K, S_1, S_2, S_3, S_4, S_5, S_6, S_7) = (1.5731, 0, 1, 3, 5, 6, 8, 10)															
0.00	500.00	495.75	30	56	115	147	181	257	348	458	601	691	802	1146	1489
0.25	32.38	28.35	5	7	10	12	14	19	24	30	38	43	50	69	89
0.50	7.41	4.31	3	3	4	4	5	5	6	7	8	9	10	13	16
0.75	3.92	1.53	2	2	3	3	3	3	4	4	4	5	5	6	7
1.00	2.75	0.85	2	2	2	2	2	2	3	3	3	3	3	4	4
1.50	1.83	0.50	1	1	1	2	2	2	2	2	2	2	2	2	3
2.00	1.28	0.45	1	1	1	1	1	1	1	1	1	2	2	2	2
n = 9, (K, S_1, S_2, S_3, S_4, S_5, S_6, S_7) = (1.1952, 0, 0, 1, 2, 3, 4, 6)															
0.00	500.00	496.99	29	55	114	146	180	257	348	459	601	692	803	1147	1492
0.25	26.46	22.88	4	6	9	10	12	15	20	25	31	35	40	56	72
0.50	5.86	3.30	2	3	3	4	4	4	5	6	7	7	8	10	12
0.75	3.03	1.30	1	2	2	2	2	3	3	3	4	4	4	5	5
1.00	2.01	0.81	1	1	1	1	2	2	2	2	2	2	3	3	3
1.50	1.18	0.39	1	1	1	1	1	1	1	1	1	1	1	2	2
2.00	1.01	0.09	1	1	1	1	1	1	1	1	1	1	1	1	1

SDRL$_1$, MRL$_1$, $\ell_{0.75} - \ell_{0.25}$ and $\ell_{0.95} - \ell_{0.05}$ when $\delta \le 0.75$. It is followed by the 7 and 4 regions RS $\bar{X}$ charts. For example, when $\delta_{\text{opt}} = 0.5$, $n = 5$ and $\delta = 0.25$, the (ARL$_1$, SDRL$_1$, MRL$_1$, $\ell_{0.75} - \ell_{0.25}$, $\ell_{0.95} - \ell_{0.05}$) are (29.66, 23.29, 23, 26, 70) (see Table 5) for the EWMA $\bar{X}$ chart as opposed to (45.89, 41.55, 33, 46, 123) (see Table 3) and (51.00, 47.01, 37, 51, 139) (see Table 1) for the 7 and 4 regions RS $\bar{X}$ charts, respectively. For $\delta_{\text{opt}} = 0.5$ (see Tables 1, 3 and 5), on the other hand, the 4 regions RS $\bar{X}$ chart generally has the fastest detection speed (i.e. the

Table 4: Exact ARL, SDRL and percentiles of the run-length distribution for the 7 regions RS $\bar{X}$ chart with optimal parameters (K, S_1, S_2, S_3, S_4, S_5, S_6, S_7), when $n \in \{3, 5, 7, 9\}$, $\delta_{\text{opt}} = 1.5$ and ARL$_0$ = 500

			Percentiles of the run-length distribution												
δ	ARL	SDRL	5th	10th	20th	25th	30th	40th	50th	60th	70th	75th	80th	90th	95th
			n = 3, (K, S_1, S_2, S_3, S_4, S_5, S_6, S_7) = (1.1233, 0, 0, 0, 2, 5, 6, 8)												
0.00	500.00	498.12	27	54	113	145	179	256	347	458	602	692	804	1149	1494
0.25	124.06	121.40	9	15	30	38	46	65	87	114	149	171	198	282	366
0.50	24.94	21.99	4	5	8	9	11	14	18	23	30	34	38	54	69
0.75	9.04	6.53	2	3	4	4	5	6	7	9	11	12	13	17	22
1.00	4.85	2.91	1	2	2	3	3	4	4	5	6	6	7	9	10
1.50	2.34	1.11	1	1	1	2	2	2	2	2	3	3	3	4	4
2.00	1.53	0.63	1	1	1	1	1	1	1	2	2	2	2	2	3
			n = 5, (K, S_1, S_2, S_3, S_4, S_5, S_6, S_7) = (1.0527, 0, 0, 0, 0, 2, 3, 5)												
0.00	500.00	499.10	27	53	112	144	179	256	347	458	602	693	804	1150	1496
0.25	112.06	110.21	7	13	26	34	41	58	78	103	135	155	179	256	332
0.50	18.89	16.45	2	4	6	7	9	11	14	18	22	25	29	40	52
0.75	6.42	4.59	1	2	3	3	4	4	5	6	8	9	9	12	15
1.00	3.31	2.06	1	1	2	2	2	2	3	3	4	4	5	6	7
1.50	1.54	0.73	1	1	1	1	1	1	1	2	2	2	2	2	3
2.00	1.10	0.30	1	1	1	1	1	1	1	1	1	1	1	1	2
			n = 7, (K, S_1, S_2, S_3, S_4, S_5, S_6, S_7) = (1.2433, 0, 0, 0, 0, 1, 2, 2)												
0.00	500.00	499.26	26	53	112	144	179	256	347	458	602	693	804	1150	1496
0.25	104.53	103.27	7	12	24	31	38	54	73	96	126	144	167	239	311
0.50	16.33	14.40	2	3	5	6	7	10	12	15	20	22	25	35	45
0.75	5.20	3.91	1	1	2	2	3	3	4	5	6	7	8	10	13
1.00	2.54	1.66	1	1	1	1	1	2	2	3	3	3	4	5	6
1.50	1.22	0.47	1	1	1	1	1	1	1	1	1	1	1	2	2
2.00	1.01	0.12	1	1	1	1	1	1	1	1	1	1	1	1	1
			n = 9, (K, S_1, S_2, S_3, S_4, S_5, S_6, S_7) = (1.0331, 0, 0, 0, 0, 0, 1, 2)												
0.00	500.00	499.31	26	53	112	144	179	256	347	458	602	693	804	1150	1496
0.25	87.00	85.87	5	10	20	26	32	45	61	80	105	120	139	199	258
0.50	12.58	10.91	1	2	4	5	6	7	10	12	15	17	19	27	34
0.75	3.98	2.97	1	1	2	2	2	3	3	4	5	5	6	8	10
1.00	1.97	1.22	1	1	1	1	1	1	2	2	2	3	3	4	4
1.50	1.08	0.29	1	1	1	1	1	1	1	1	1	1	1	1	2
2.00	1.00	0.04	1	1	1	1	1	1	1	1	1	1	1	1	1

smallest ARL_1 value) among all the three charts under comparison when $\delta \geq 1.0$. However, the $SDRL_1$ value for the EWMA $\bar{X}$ chart is generally the smallest compared to the 4 and 7 regions RS $\bar{X}$ charts when $\delta \geq 1.0$. Regarding the MRL_1, $\ell_{0.75} - \ell_{0.25}$ and $\ell_{0.95} - \ell_{0.05}$, the three charts have about the same performance when $\delta \geq 1.0$.

Let us focus on Tables 2, 4 and 6 when $\delta_{opt} = 1.5$. Here, we observe that the EWMA $\bar{X}$ chart generally has the worst performances compared to the 4 and 7 regions RS $\bar{X}$ charts, for all sizes of mean shifts when $n \in \{5, 7\}$; while for $n \in \{3, 9\}$, the 4 regions RS $\bar{X}$ chart is

Table 5: Exact ARL, SDRL and percentiles of the run-length distribution for the EWMA $\bar{X}$ chart with optimal parameters (λ, H), when $n \in \{3, 5, 7, 9\}$, $\delta_{opt} =$ 0.5 and ARL_0 = 500

			Percentiles of the run-length distribution												
δ	ARL	SDRL	5th	10th	20th	25th	30th	40th	50th	60th	70th	75th	80th	90th	95th
$n = 3$, $(\lambda, H) = (0.1090, 0.3931)$															
0.00	500.00	492.45	33	59	116	148	181	256	345	454	593	682	791	1128	1465
0.25	41.69	32.83	9	12	16	19	21	26	32	39	49	55	62	84	107
0.50	12.71	6.69	5	6	7	8	9	10	11	13	15	16	17	21	26
0.75	7.18	2.83	4	4	5	5	5	6	7	7	8	9	9	11	13
1.00	5.03	1.63	3	3	4	4	4	4	5	5	6	6	6	7	8
1.50	3.23	0.82	2	2	3	3	3	3	3	3	4	4	4	4	5
2.00	2.43	0.55	2	2	2	2	2	2	2	3	3	3	3	3	3
$n = 5$, $(\lambda, H) = (0.1594, 0.3842)$															
0.00	500.00	493.67	31	57	115	146	180	255	345	454	595	684	793	1132	1472
0.25	29.66	23.29	6	8	12	13	15	19	23	28	35	39	44	60	76
0.50	8.60	4.35	4	4	5	6	6	7	8	9	10	11	12	14	17
0.75	4.86	1.81	3	3	3	4	4	4	5	5	5	6	6	7	8
1.00	3.44	1.05	2	2	3	3	3	3	3	4	4	4	4	5	5
1.50	2.27	0.52	2	2	2	2	2	2	2	2	2	3	3	3	3
2.00	1.83	0.41	1	1	2	2	2	2	2	2	2	2	2	2	2
$n = 7$, $(\lambda, H) = (0.2041, 0.3779)$															
0.00	500.00	495.62	30	56	114	146	180	256	346	455	597	687	797	1138	1479
0.25	23.63	18.53	5	7	9	11	12	15	18	22	28	31	35	48	60
0.50	6.63	3.27	3	3	4	4	5	5	6	7	8	8	9	11	13
0.75	3.77	1.36	2	2	3	3	3	3	4	4	4	4	5	6	6
1.00	2.70	0.79	2	2	2	2	2	2	3	3	3	3	3	4	4
1.50	1.86	0.45	1	1	2	2	2	2	2	2	2	2	2	2	2
2.00	1.35	0.48	1	1	1	1	1	1	1	1	2	2	2	2	2
$n = 9$, $(\lambda, H) = (0.2445, 0.3726)$															
0.00	500.00	496.77	29	56	114	146	180	256	346	456	598	689	799	1141	1484
0.25	19.89	15.58	4	6	8	9	10	12	15	19	23	26	29	40	51
0.50	5.46	2.64	2	3	3	4	4	4	5	5	6	7	7	9	11
0.75	3.12	1.09	2	2	2	2	2	3	3	3	3	4	4	5	5
1.00	2.27	0.63	1	2	2	2	2	2	2	2	2	3	3	3	3
1.50	1.53	0.51	1	1	1	1	1	1	2	2	2	2	2	2	2
2.00	1.08	0.27	1	1	1	1	1	1	1	1	1	1	1	1	2

generally the worst among all the three control charts. Still investigating Tables 2, 4 and 6, when $\delta \le 0.75$ and $n \in \{3, 9\}$, the ARL₁, SDRL₁, MRL₁, $\ell_{0.75} - \ell_{0.25}$ and $\ell_{0.95} - \ell_{0.05}$ for the 7 regions RS $\bar{X}$ chart are the smallest among all the three charts under comparison; while these performance measures are the smallest for the 4 regions RS $\bar{X}$ chart when $n \in \{5, 7\}$. For $\delta \ge 1.0$, the 7 regions RS $\bar{X}$ chart outperforms the 4 regions RS $\bar{X}$ and EWMA $\bar{X}$ charts, in terms of ARL_1 and $SDRL_1$ (see Tables 2, 4 and 6). Similarly, all the three charts have competitive performances, in terms of the MRL_1, $\ell_{0.75} - \ell_{0.25}$ and $\ell_{0.95} - \ell_{0.05}$, when $\delta \ge 1.0$.

Table 6: Exact ARL, SDRL and percentiles of the run-length distribution for the EWMA $\bar{X}$ chart with optimal parameters (λ, H), when $n \in \{3, 5, 7, 9\}$, $\delta_{opt} =$ 1.5 and ARL_0 = 500

			Percentiles of the run-length distribution												
δ	ARL	SDRL	5th	10th	20th	25th	30th	40th	50th	60th	70th	75th	80th	90th	95th
$n = 3$, $(\lambda, H) = (0.5495, 1.0932)$															
0.00	500.00	498.33	27	54	112	145	179	256	346	457	601	691	802	1147	1492
0.25	127.88	125.96	8	15	30	38	47	66	89	117	153	176	205	292	379
0.50	28.14	26.13	3	5	8	10	11	15	20	26	33	38	44	62	80
0.75	9.92	8.05	2	3	4	4	5	6	8	9	12	13	15	20	26
1.00	5.02	3.38	2	2	2	3	3	3	4	5	6	6	7	9	12
1.50	2.35	1.11	1	1	2	2	2	2	2	2	3	3	3	4	4
2.00	1.56	0.63	1	1	1	1	1	1	1	2	2	2	2	2	3
$n = 5$, $(\lambda, H) = (0.7664, 1.0885)$															
0.00	500.00	499.39	26	53	112	144	179	256	347	458	602	693	804	1150	1496
0.25	118.52	117.43	7	13	27	35	43	61	82	109	142	164	190	271	353
0.50	23.53	22.35	2	4	6	8	9	13	17	22	28	32	37	53	68
0.75	7.48	6.35	1	2	3	3	3	4	6	7	9	10	11	16	20
1.00	3.51	2.50	1	1	2	2	2	2	3	3	4	5	5	7	8
1.50	1.56	0.75	1	1	1	1	1	1	1	2	2	2	2	2	3
2.00	1.10	0.31	1	1	1	1	1	1	1	1	1	1	1	1	2
$n = 7$, $(\lambda, H) = (0.8834, 1.0387)$															
0.00	500.00	499.30	26	53	112	144	179	256	346	458	602	693	804	1150	1496
0.25	106.21	105.45	6	12	24	31	38	55	74	97	128	147	170	244	317
0.50	19.32	18.49	2	3	5	6	7	10	14	18	23	26	31	43	56
0.75	5.77	4.96	1	1	2	2	3	3	4	5	7	8	9	12	16
1.00	2.63	1.87	1	1	1	1	1	2	2	2	3	3	4	5	6
1.50	1.22	0.49	1	1	1	1	1	1	1	1	1	1	1	2	2
2.00	1.01	0.12	1	1	1	1	1	1	1	1	1	1	1	1	1
$n = 9$, $(\lambda, H) = (0.9415, 0.9714)$															
0.00	500.00	499.25	26	53	112	144	179	256	347	458	602	693	804	1150	1496
0.25	92.15	91.53	5	10	21	27	33	47	64	84	111	128	148	211	275
0.50	15.39	14.72	1	2	4	5	6	8	11	14	18	21	24	35	45
0.75	4.44	3.78	1	1	2	2	2	3	3	4	5	6	7	9	12
1.00	2.04	1.38	1	1	1	1	1	1	2	2	2	3	3	4	5
1.50	1.09	0.30	1	1	1	1	1	1	1	1	1	1	1	1	2
2.00	1.00	0.04	1	1	1	1	1	1	1	1	1	1	1	1	1

From Tables 1 to 6, when $\delta \leq 0.75$, it is found that the detection speed and variation of the run-length distribution of the three control charts specially designed for $\delta_{\text{opt}} = 0.5$ (see Tables 1, 3 and 5) is faster than those designed for $\delta_{\text{opt}} = 1.5$ (see Tables 2, 4 and 6). For example, the (ARL_1, SDRL_1, MRL_1, $\ell_{0.75} - \ell_{0.25}$, $\ell_{0.95} - \ell_{0.05}$) values for the 7 regions RS $\bar{X}$ chart are (10.18, 6.70, 8, 7, 20) when $\delta_{\text{opt}} = 0.5$, $n = 5$ and $\delta = 0.50$ (see Table 3). These (ARL_1, SDRL_1, MRL_1, $\ell_{0.75} - \ell_{0.25}$, $\ell_{0.95} - \ell_{0.05}$) values for the 7 regions RS $\bar{X}$ chart when $\delta_{\text{opt}} = 1.5$, $n = 5$ and $\delta = 0.50$ are larger than those for $\delta_{\text{opt}} = 0.5$, i.e. (18.89, 16.45, 14, 18, 50) (see Table 4). On the contrary, for $\delta \geq 1.0$, the three control charts specially designed for $\delta_{\text{opt}} = 1.5$ (see Tables 2, 4 and 6) surpass those designed for $\delta_{\text{opt}} = 0.5$ (see Tables 1, 3 and 5). This implies that the control charts optimized based on $\delta_{\text{opt}} = 0.5$ are more effective in detecting small shifts; while those optimized based on $\delta_{\text{opt}} = 1.5$ are more suitable for detecting large shifts.

5. Conclusion

In this paper, we demonstrate that the ARL is a peculiar performance measure. Therefore, dependence on the ARL measure alone is discouraged. On the contrary, the percentiles of the run-length distribution which provide the exact behaviour of the run-length distribution of a control chart, are more intuitive. To have an in-depth knowledge and high confidence of a control chart, it is necessary to investigate a control chart, in terms of the ARL, SDRL and percentiles of the run-length distribution. Hence, in this paper, we provide a thorough investigation of the exact run-length properties of the RS $\bar{X}$ and EWMA $\bar{X}$ charts.

The comparative results reveal that the 7 regions RS $\bar{X}$ charts which are optimized with respect to $\delta_{\text{opt}} = 1.5$, outshine the corresponding EWMA $\bar{X}$ chart for all sizes of shifts. When all the three control charts are optimally designed with respect to $\delta_{\text{opt}} = 0.5$, the EWMA $\bar{X}$ chart is the best in detecting small mean shifts ($\delta \leq 0.75$) and has the smallest variation of the run-length distribution for all levels of shift sizes. The percentiles of the run-length distribution change with n and δ_{opt} (see Tables 1 to 6), even though the same value of ARL_0 is attained. For detecting small mean shifts, it is recommended to design a control chart based on a small optimal shift size and vice versa.

Acknowledgements

This research is supported by the Universiti Tunku Abdul Rahman, Fundamental Research Grant Scheme (FRGS) no. FRGS/1/2015/SG04/UTAR/02/3.

References

Abdul H., Jennifer B. & Elena M. 2015. A new exponentially weighted moving average control chart for monitoring the process mean. *Quality and Reliability Engineering International* **31**(8): 1623-1640.

Acosta-Mejia C.A. & Pignatiello J.J.Jr. 2010. The run sum *R* chart with fast initial response. *Communications in Statistics-Simulation and Computation* **39**(5): 921-932.

Acosta-Mejia C.A. & Rincon L. 2014. The continuous run sum chart. *Communications in Statistics-Theory and Methods* **43**(20): 4371-4383.

Aguirre-Torres V. & Reyes-Lopez D. 1999. Run sum charts for both $\bar{X}$ and *R*. *Quality Engineering* **12**(1): 7-12.

Bischak D.P. & Trietsch D. 2007. The rate of false signals in $\bar{X}$ control charts with estimated limits. *Journal of Quality Technology* **39**(1): 54-65.

Castagliola P., Celano G. & Psarakis S. 2011. Monitoring the coefficient of variation using EWMA charts. *Journal of Quality Technology* **43**(3): 249-265.
Chakraborti S. 2007. Run length distribution and percentiles: The Shewhart $\bar{X}$ chart with unknown parameters. *Quality Engineering* **19**(2): 119-127.
Champ C.W. & Rigdon S.E. 1997. An analysis of the run sum control chart. *Journal of Quality Technology* **29**(4): 407-417.
Crowder S.V. 1987. Average run length of exponentially weighted moving average control charts. *Journal of Quality Technology* **19**(3): 161-164.
Crowder S.V. 1989. Design of exponentially weighted moving average schemes. *Journal of Quality Technology* **21**(3): 155-162.
Davis R.B., Jin C. & Guo Y. 1994. Improving the performance of the zone control chart. *Communications in Statistics-Theory Methods* **23**(12): 3557-3565.
Davis R.B. & Krehbiel T.C. 2002. Shewhart and zone control chart performance under linear trend. *Communications in Statistics-Simulation and Computation* **31**(1): 91-96.
Gan F.F. 1993. An optimal design of EWMA control charts based on median run length. *Journal of Statistical Computation and Simulation* **45**(3): 169-184.
Jaehn A. H. 1987. Zone control chart-SPC made easy. *Quality* **26**: 51-53.
Jones L.A. 2002. The statistical design of EWMA control charts with estimated parameters. *Journal of Quality Technology* **34**(3): 277-288.
Khan N., Aslam M. & Jun C.H. 2016. A EWMA control chart for exponential distributed quality based on moving average statistics. *Quality and Reliability Engineering International* **32**(3): 1179-1190.
Khoo M.B.C., Castagliola P., Liew J.Y., Teoh W.L. & Maravelakis P.E. 2016. A study on EWMA charts with runs rules-The markov chain approach. *Communications in Statistics-Theory and Methods* **45**(14): 4156-4180.
Khoo M.B C. 2004. Performance measures for the Shewhart $\bar{X}$ control chart. *Quality Engineering* **16**(4): 585-590.
Khoo M.B.C. & Quah S.H. 2002. Computing the percentage points of the run-length distributions of multivariate CUSUM control charts. *Quality Engineering* **15**(2): 299-310.
Lucas J.M. & Saccucci M.S. 1990. Exponentially weighted moving average control schemes: Properties and enhancements. *Technometrics* **32**(1): 1-29.
Montgomery D.C. 2013. *Statistical Quality Control: A Modern Introduction*. 7th Ed. New York: John Wiley & Sons.
Palm A.C. 1990. Tables of run length percentiles for determining the sensitivity of Shewhart control chart for averages with supplementary runs rules. *Journal of Quality Technology* **22**(4): 289-298.
Parkhideh S. & Parkhideh B. 1998. Design of a flexible zone individuals control chart. *International Journal of Production Research* **36**(8): 2259-2267.
Radson D. & Boyd A.H. 2005. Graphical representation of run length distributions. *Quality Engineering* **17**(2): 301-308.
Reynolds J.H. 1971. The run sum control chart procedure. *Journal of Quality Technology* **3**(1): 23-27.
Roberts S.W. 1959. Control chart tests based on geometric moving averages. *Technometrics* **1**(3): 239-250.
Roberts S.W. 1966. A comparison of some control chart procedures. *Technometrics* **8**(3): 411-430.
Shu L.J., Jiang W. & Wu S.J. 2007. A one-sided EWMA control chart for monitoring process means. *Communication in Statistics-Simulation and Computation* **36**(4): 901-920.
Shmueli G. & Cohen A. 2003. Run-length distribution for control charts with runs and scans rules. *Communitation in Statistics-Theory and Methods* **32**(2): 475-495.
Sitt C.K., Khoo M.B.C., Shamsuzzaman M. & Chen C.H. 2014. The run sum *t* control chart for monitoring process mean changes in manufacturing. *International Journal of Advanced Manufacturing Technology* **70**(5):148-1504.
Steiner S.H. 1999. EWMA control charts with time-varying control limits and fast initial response. *Journal of Quality Technology* **31**(1): 75-86.
Teoh W.L., Khoo M.B.C., Castagliola P. & Chakraborti S. 2015. A median run length-based double-sampling $\bar{X}$ chart with estimated parameters for minimizing the average sample size. *International Journal of Advanced Manufacturing Technology* **80**(1): 411-426.
Teoh W.L., Khoo M.B.C., Castagliola P. & Lee M.H. 2016. The exact run length distribution and design of the Shewhart $\bar{X}$ chart with estimated parameters based on median run length. *Communications in Statistics-Simulation and Computation* **45**(6): 2081-2103.
Teoh W.L., Khoo M.B.C., Castagliola P., Yeong W.C. & Teh S.Y. 2017. Run-sum control charts for monitoring the coefficient of variation. *European Journal of Operational Research* **257**(1): 144-158.
Zhang L., Chen G. & Castagliola P. 2009. On *t* and EWMA *t* charts for monitoring changes in the process mean. *Quality and Reliability Engineering International* **25**(8): 933-945.

[1]*Department of Physical and Mathematical Science*
Faculty of Science
Universiti Tunku Abdul Rahman
31900 Kampar, Perak, MALAYSIA
E-mail: cjk_890116@hotmail.com, teohwl@utar.edu.my, chongzl@utar.edu.my*

[2]*School of Mathematical Sciences*
Universiti Sains Malaysia
11800 Penang, MALAYSIA
E-mail: mkbc@usm.my

[3]*School of Management*
Universiti Sains Malaysia
11800 Penang, MALAYSIA
E-mail: tehsyin@usm.my

* Corresponding author